

ND-R167 555

GENERATION OF SPIRAL BEVEL GEARS WITH ZERO KINEMATICAL
ERRORS AND COMPUTE. (U) NATIONAL AERONAUTICS AND SPACE
ADMINISTRATION CLEVELAND OH LE. F L LITVIN ET AL.

1/1

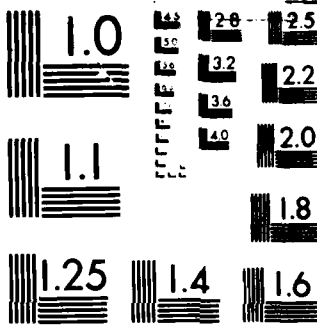
UNCLASSIFIED

MAR 86 NASA-E-2932 NASA-TM-87273

F/G 13/9

NL





MICROCOPY RESOLUTION TEST CHART
NATIONAL BUREAU OF STANDARDS-1963-A

2

NASA
Technical Memorandum 87273

USAAVSCOM
Technical Report 86-C-2

Generation of Spiral Bevel Gears With Zero Kinematical Errors and Computer Aided Tooth Contact Analysis

Faydor L. Litvin and Wei-Jiung Tsung
University of Illinois at Chicago
Chicago, Illinois

and

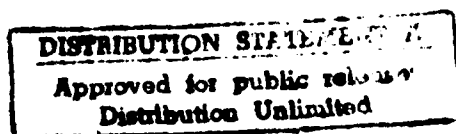
John J. Coy
Propulsion Directorate
U.S. Army Aviation Research and Technology Activity—AVSCOM
Lewis Research Center
Cleveland, Ohio

and

Charles Heine
Dana Corporation
Fort Wayne, Indiana

March 1986

NASA



DTIC
ELECTE
MAY 12 1986
S D

06 5 12 100

AD-A167 555

GENERATION OF SPIRAL BEVEL GEARS WITH ZERO KINEMATICAL ERRORS AND COMPUTER
AIDED TOOTH CONTACT ANALYSIS

Faydor L. Litvin and Wei-Jiung Tsung
University of Illinois at Chicago
Department of Mechanical Engineering
Chicago, Illinois

John J. Coy
Propulsion Directorate
U.S. Army Aviation Research and Technology Laboratories - AVSCOM
Lewis Research Center
Cleveland, Ohio

and

Charles Heine
Dana Corporation
Fort Wayne, Indiana

SUMMARY

A new method for the generation of Gleason's spiral bevel gears which provides conjugated gear tooth surfaces and an improved bearing contact has been developed. A computer aided program for the simulation of meshing, misalignment, and bearing contact has been developed.

INTRODUCTION

The area of geometry and generation of spiral bevel gears has been a subject of intensive research for many authors. Litvin and his co-authors have addressed analysis and synthesis of spiral bevel gears (refs. 1 to 5). Computer aided simulations of tooth meshing and contact have been worked out by Litvin and Gutman (refs. 6 and 7) and by the Gleason works (refs. 8 and 9).

For many years, the Gleason Works has provided the machinery for manufacture of spiral bevel gears (ref. 10). There are several important advantages to the Gleason methods of manufacture over hobbing methods. The machines are rigid and produce gears of high quality and consistency. The cutting methods may be used for both milling and grinding. Grinding is especially important for producing hardened high quality aircraft gears. Both milling and grinding are possible with Gleason's method. The velocity of the cutting wheel does not have to be related in any way with the machine's generating motions. A dis-

advantage is that this method does not produce conjugate gear tooth surfaces. This means that the gear ratio is not constant during the tooth engagement cycle, and therefore, there are kinematical errors in the transformation of rotation from the driving gear to the driven gear.

The kinematic errors in spiral bevel gears are a major source of noise and vibrations in transmissions. Vibration tests on a helicopter transmission have been conducted by the NASA Lewis Research Center (ref. 11). Figure 1 shows the vibration measured by placing an accelerometer on a transmission housing. The bevel gear mesh caused the most noise and vibration. By comparison, the planetary spur gear stage was relatively quiet.

Therefore, the objective of the research presented herein was to find a way to eliminate the kinematic errors for bevel gears and to improve the conditions of lubrication and the bearing contact, while retaining all the advantages of the Gleason system of manufacturing such gears. The solution to this problem is based on a new method for generation of conjugate gear tooth surfaces which is proposed by the authors. This method can be applied using the existing Gleason machines and tools with specially calculated machine tool settings determined by the new method. The new method for generation provides a localized bearing contact which is typical for Gleason's gears and is necessary to reduce the sensitivity of the gear tooth surface contact to misalignments and deflections of gear shafts under operating conditions. In the past, a computer-aided tooth contact analysis was used to obtain improved gear contacts and kinematic errors by using a trial and error search through the possible machine tool settings. Settings found this way were only partially successful at reducing kinematic errors because the gears did not have conjugate tooth surfaces.

The new method for determination of machine tool settings does not need such a search and directly provides the settings for the generation of spiral bevel gears with zero kinematical errors. The new tooth contact analysis computer program that was written provides the information on the localized tooth bearing contact, the influence of misalignment, and the kinematic errors. This new computer program was used to verify the improved gear machine settings.

NOMENCLATURE

| | |
|--|---|
| \underline{a} | unit vector along pitch line (fig. 5) |
| b_F, b_p | parameters of pinion and gear machine-tool setting (fig. 2), cm (in.) |
| $\underline{i}_I^{(1)}, \underline{i}_I^{(2)}$ | unit vectors of principal pinion and gear direction (fig. 8) |
| K_n | normal curvature cm^{-1} (in. ⁻¹) |
| $K_I^{(1)}, K_{II}^{(1)}$ | pinion principal curvatures, cm^{-1} (in. ⁻¹) |
| $K_I^{(2)}, K_{II}^{(2)}$ | gear principal curvatures, cm^{-1} (in. ⁻¹) |
| M | main contact point of gear (fig. 3) |
| m_{12} | gear ratio: $m_{12} = \omega^{(1)}/\omega^{(2)}$ |
| N | main contact point of pinion (fig. 4) |
| \underline{N} | common normal to surfaces at current contact point (figs. 5 and 6) |
| $\underline{n}^{(F)}$ | pinion generator tooth surface unit normal |
| $\underline{n}_f^{(1)}$ | unit vector normal to tooth surface ($i = 1, 2$) expressed in coordinate frame S_f |
| P | current contact point (figs. 5 and 6) |
| q_F, q_p | parameters of pinion and gear machine-tool settings (fig. 2), radians |
| $r_c^{(F)}, r_c^{(P)}$ | theoretical radius of the generating surface measured in plane $x_m^{(i)} = 0$ ($i = 1, 2$) (fig. 2), cm (in.) |
| $\underline{r}_f^{(1)}$ | position vector for a contact point on tooth surface ($i = 1, 2$), expressed in coordinate frame S_f , cm (in.) |
| u_F, u_p | generating cones surface coordinates (fig. 2) |
| $\underline{v}^{(F)}$ | surface Σ_F contact point velocity, cm/sec (in./sec) |
| $\underline{v}^{(1)}$ | surface Σ_1 contact point velocity, cm/sec (in./sec) |
| $2a, 2b$ | major and minor axes of contact ellipse (fig. 8), mm (in.) |
| α | orientation angle of contact ellipse (fig. 8), rad |
| β_F, β_p | pinion, gear spiral bevel angle, deg |
| γ_1, γ_2 | pinion, gear pitch angle, deg |

| | |
|-------|-------------------------------------|
| For | |
| CRA&I | <input checked="" type="checkbox"/> |
| TAB | <input type="checkbox"/> |
| anced | <input type="checkbox"/> |
| tion | |

| | |
|--------------------|----------------------|
| Distribution / | |
| Availability Codes | |
| Dist | Avail and/or Special |
| A-1 | |

| | |
|------------------------------|--|
| $\Delta E_1, \Delta L_1$ | machine-tool setting corrections (fig. 4), mm (in.) |
| Δ_1, Δ_2 | pinion, gear dedendum angle, deg |
| δ | rotation of frame S_h relative to frame S_f about axis Z_1 , rad |
| δ_e | surface elastic approach, mm (in.) |
| θ_F, θ_P | generating cones surface coordinates (fig. 2), rad |
| Σ_1, Σ_2 | pinion and gear tooth surfaces |
| Σ_F, Σ_P | generating surfaces for pinion and gear |
| $\sigma(21)$ | angle formed by unit vectors $\underline{i}_I^{(2)}$ and $\underline{i}_I^{(1)}$ (fig. 8), rad |
| φ_F, φ_P | generating surfaces rotation angles (fig. 2), rad |
| φ_1', φ_2' | pinion, gear rotation angle, rad |
| $\psi_c^{(F)}, \psi_c^{(P)}$ | head cutters blade angles for pinion and gear (fig. 2), deg |
| $\omega^{(F)}, \omega^{(P)}$ | cradle angular velocities for cutting the pinion and gear, rad/sec |
| $\omega^{(1)}, \omega^{(2)}$ | pinion and gear angular velocities, rad/sec |

Subscript, superscripts:

| | |
|---|----------------------|
| c | cradle |
| F | pinion generator |
| m | machine |
| P | gear generator |
| s | surface of generator |
| 1 | pinion |
| 2 | gear |

Cartesian coordinate frames:

| | |
|-------------|---|
| $S_c^{(j)}$ | connected to cradle $j = F, P$ |
| S_f | fixed to frame of gearbox, used for mesh of Σ_1 and Σ_2 |
| S_h | fixed to machine, used for mesh of Σ_F and Σ_1 |
| $S_m^{(1)}$ | connected to machine frame $i = 1, 2$ |
| $S_s^{(j)}$ | connected to tool cone $j = F, P$ |
| S_1, S_2 | connected to pinion, gear |

MANUFACTURING METHOD

The existing method for generation of Gleason's spiral bevel gears may be described as follows. The gear cutter cuts a single space during a single index cycle. The gear cutter is mounted to the cradle of the cutting machine. The machine cradle with the cutter may be imagined as a crown gear that meshes with the gear being cut. The cradle with the mounted head cutter rotates slowly about its axis, as does the gear which is being cut. The combined process generates the gear tooth surface. The cradle only rotates far enough so that one space is cut out and then it rapidly reverses while the workpiece is withdrawn from the cutter and indexed ahead in preparation for cutting the next tooth. The desired cutter velocity is provided while the cutter spins about its axis which itself moves in a circular path.

Generating surfaces, Σ_F and Σ_P , are used for the generation of the pinion tooth surface, Σ_1 , and the gear tooth surface, Σ_2 , respectively. The generating surfaces, Σ_F and Σ_P , are cones with slightly different dimensions to localize the bearing contact. Usually both sides of the gear tooth are cut simultaneously (duplex method) but both sides of the pinion tooth are cut separately. In the process of meshing, surfaces Σ_F and Σ_1 , and respectively surfaces Σ_P and Σ_2 , contact each other at every instant at a line (contact line) which is a spatial curve. The shape of the contact line and its location on the contacting surfaces is changed in the process of meshing. The generated pinion and gear tooth surfaces are in contact at a point (contact point) at every instant.

Figure 2 shows the cone-surface which is the generating tool surface. We consider two coordinate systems rigidly connected to the cradle: (1) $S_S^{(j)}$ in which we represent the cone surface and (2) $S_C^{(j)}$ which is rigidly connected to $S_S^{(j)}$ and rotates about the $x_m^{(1)}$ - axis of the fixed coordinate systems $S_m^{(1)}$ ($j = F, P; i = 1, 2$). The cradle with the cone surface represents the generating gear which is in mesh with the pinion (gear) in the process of cutting. The cone surface represents the tooth surface of the imaginary generating gear.

The generating surfaces are represented in $S_C^{(j)}$ ($j = F, P$) by the following equations:

$$\begin{aligned}
x_c^{(j)} &= r_c^{(j)} \cot \psi_c^{(j)} - u_j \cos \psi_c^{(j)} \\
y_c^{(j)} &= u_j \sin \psi_c^{(j)} \sin (\theta_j \mp q_j) \mp b_j \sin q_j \\
z_c^{(j)} &= u_j \sin \psi_c^{(j)} \cos (\theta_j \mp q_j) + b_j \cos q_j \\
(j &= F, P)
\end{aligned}
\tag{1}$$

Here: u_j , θ_j are the generating surface coordinates; b_j and q_j are the parameters of machine-tool settings; $r_c^{(j)}$ is the head-cutter radius which is measured in plane $x_m^{(1)} = 0$; and the upper and lower signs for q_j in equations (1) are given for the left-hand and right-hand spiral gears, respectively.

We consider the generation of the gear (member 2) and the pinion (member 1) separately; first the gear, then the pinion. Considering the generation of the gear (fig. 3), we use the following coordinate systems: (1) $S_c^{(P)}$, a movable coordinate system, which is rigidly connected to the generating gear (to the cradle with the generating surface Σ_p) and (2) a fixed coordinate system $S_m^{(2)}$ which is rigidly connected to the frame of the cutting machine, and the coordinate system S_2 which is rigidly connected to gear 2. The location of coordinate $S_s^{(P)}$ with respect to $S_c^{(P)}$ is determined by q_p and b_p , (fig. 2). φ_p represents the cradle rotation, $r_c^{(P)}$ is the radius of the head cutter circle, and β_p is the root cone spiral angle.

The cradle of the cutting machine carries the head-cutter (fig. 3). The cradle rotates about the $x_m^{(2)}$ coordinate axis with angular velocity $\omega^{(P)}$ while the gear being generated rotates about its axis z_2 with angular velocity $\omega^{(2)}$. The angular velocities of cradle and gear are related by ratio $m_{2p} = \omega^{(2)}/\omega^{(P)}$. Axis $x_m^{(2)}$ is perpendicular to the gear root cone (fig. 3). Thus, axes z_2 and $z_m^{(2)}$ make the angle $\gamma_2 - \Delta_2$, where γ_2 is the pitch angle and Δ_2 is the gear dedendum angle.

An auxiliary fixed coordinate system S_f is rigidly connected to the housing of the gear train. We will consider the meshing of gears 1 and 2 in system S_f .

Similarly, considering the pinion generation, we use the coordinate systems $S_s^{(F)}$ and $S_c^{(F)}$ (fig. 2), $S_m^{(1)}$ and S_1 (fig. 4). We designate

S_h to be an auxiliary fixed coordinate system, where we consider the mesh of surfaces Σ_f and Σ_1 . Coordinate systems S_h and S_f are related by having a common origin and a small relative angular displacement, δ .

Unlike for the generation of gear 2, the axes of rotation $x_m^{(1)}$ and z_1 do not intersect each other; rather they cross, and ΔE_1 and ΔL_1 are the sought-for corrections of the machine-tool settings with which the meshing of gears 1 and 2 is to be improved. In addition, two other parameters must be determined. They are the blade angle $\psi_c^{(F)}$ and a turning angle δ which determines the orientation of coordinate frame S_h with respect to S_f . This turning is performed about the pinion axis, z_1 , when the gear and pinion will have been placed in mesh and with the origins O_h and O_f being coincident.

THE NEW GENERATION METHOD

Figure 5 shows plane Π which is defined by the normal to the tool cone surface at the main contact point P and the pitch line which is the line of tangency of the pitch cones. The pitch line is the instantaneous axis of rotation of the bevel gears.

Let us consider the meshing of surfaces Σ_f , Σ_p , Σ_1 , and Σ_2 in plane Π (fig. 6). Plane Π intersects the gear and pinion generating surfaces (tool cones), Σ_p and Σ_f , forming curves L_p and L_f , respectively. Each tool cone axis is perpendicular to its generated gear root cone and the axes of the tool cones are crossed (i.e., nonparallel and nonintersecting). Surfaces Σ_p and Σ_f are tangent at point P . However, they interfere with each other within the neighborhood of point P because the tool cone axes are crossed. Points C and A , respectively, represent the intersection of the gear and pinion generating tool cone axes with plane Π . For each tool cone, every surface normal passes through the cone axis. Therefore the common normals to surfaces Σ_p and Σ_f , which, by definition, lie in plane Π , must pass through points C and A , respectively. Plane Π intersects the cradle axis of the gear cutting machine at point O . Likewise, the cradle axis of the pinion intersects plane Π at D . During the processes of meshing, the point of contact, P , shall be constrained to move in plane Π as the cradles are rotated about their axes. The equation of meshing for the generating surfaces Σ_p and Σ_f is as follows (refs. 1 and 2)

$$\left(\underline{v}^{(P)} - \underline{v}^{(F)} \right) \cdot \underline{N} = \left\{ \left(\underline{\omega}^{(P)} - \underline{\omega}^{(F)} \right) \times \underline{r}^{(M)} - \overline{OD} \times \underline{\omega}^{(F)} \right\} \cdot \underline{N} = 0 \quad (2)$$

where $\underline{v}^{(P)}$ and $\underline{v}^{(F)}$ are the velocities of the common point P of the surfaces Σ_P and Σ_F ; $\underline{\omega}^{(P)}$ and $\underline{\omega}^{(F)}$ are the angular velocities of rotation for the cradles; \underline{N} is the common normal to the tool cone surfaces; and $\underline{r}^{(M)} = \overline{OP}$.

Assume that the sought for machine tool corrections, ΔE_1 and ΔL_1 (fig. 4) will provide that \overline{OD} is parallel to \underline{N} at the starting position of the tool cones. Then equation (2) can be simplified to the following:

$$\left[\left(\underline{\omega}^{(P)} - \underline{\omega}^{(F)} \right) \times \underline{r}^{(M)} \right] \cdot \underline{N} = 0 \quad (3)$$

If we interpret equation (3) geometrically, it requires that vectors $(\underline{\omega}^{(P)} - \underline{\omega}^{(F)})$, $\underline{r}^{(M)}$, and \underline{N} have to lie in the same plane, which in this case is plane Π . In equation (3), $\underline{r}^{(M)}$ is as yet unknown, so we may substitute another vector which lies in plane Π , namely \underline{a} , which is the unit vector directed along the pitch line. (The pitch line is the line of tangency between the pitch cones of the gear and pinion.) Then the equation of meshing may be written as follows

$$\left[\left(\underline{\omega}^{(P)} - \underline{\omega}^{(F)} \right) \times \underline{a} \right] \cdot \underline{N} = 0 \quad (4)$$

Using the same approach, the equation for meshing between the surfaces Σ_1 and Σ_2 is

$$\left[\left(\underline{\omega}^{(1)} - \underline{\omega}^{(2)} \right) \times \underline{a} \right] \cdot \underline{N} = 0 \quad (5)$$

Likewise, for surfaces Σ_F and Σ_1

$$\left[\left(\underline{\omega}^{(F)} - \underline{\omega}^{(1)} \right) \times \underline{a} \right] \cdot \underline{N} = 0 \quad (6)$$

Because the three pairs of surfaces (Σ_P and Σ_F , Σ_1 and Σ_2 , and Σ_F and Σ_1) are in mesh at point P, then it must also be true that all surfaces Σ_1 , Σ_2 , Σ_F , Σ_P are in mesh at point P.

Of course since \underline{a} is in the direction of the pitch line, and since, by definition, the pitch line is the instantaneous axis of relative rotation between the pitch cones of the pinion and gear, $\underline{\omega}^{(1)} - \underline{\omega}^{(2)}$, then equation (5)

is directly satisfied. Another way to understand that equation (5) is satisfied is as follows. Meshing contact of Σ_1 and Σ_2 at P is guaranteed since the normal \underline{N} intersects the pitch line. This condition exactly satisfies the fundamental law of toothed gearing. Therefore Σ_1 and Σ_2 are in mesh at P, and furthermore there will be conjugate action between the pinion and gear (i.e., constancy of gear ratio).

Let us remember that equations (4) and (6) are valid in the process of meshing of the surfaces Σ_p , Σ_f , Σ_1 , and Σ_2 only if the normal \underline{N} remains parallel to \overline{OD} . Thus the new method of generation must provide that as \underline{N} translates (or equivalently as \overline{CA} translates) it must remain parallel to \overline{OD} . Next, let us consider how we can accomplish such a motion for link CA, imagining that OCAD is a mechanism.

Figure 7(a) shows a well-known case where the parallel motion of a straight line can be provided just by an ordinary parallelogram. Figure 7(b) shows that a parallel motion of a straight line may be performed by two equal ellipses having the same orientation. A more general case is shown in figure 7(c). We have found that a parallel motion for link CA may be performed by two mating ellipses of different dimensions and orientation. The relations between the mating ellipses is the basis for the determination of machine-tool settings for generation of conjugate tooth surfaces for spiral bevel gears. The mating ellipses are traced out by points C and A when the cradles are rotated about their axes which pass through O and D, respectively.

TOOTH CONTACT ANALYSIS

Kinematic Errors

A Tooth Contact Analysis Computer program was developed to provide numerical results that check the theory that was derived to minimize the kinematic errors. The TCA program calculates tooth bearing contact, contact path, and kinematic errors as a result of the input, which includes the machine settings and any misalignments. The program is based on the following principle. At the instantaneous contact point between the meshing teeth, the position vectors must agree, the equations for meshing between generator and generated gear must be obeyed, and the surface normals must agree. The following equations represent these principles.

$$\underline{r}_f^{(1)}(u_F, \theta_F, \varphi_F, \varphi_1') = \underline{r}_f^{(2)}(u_P, \theta_P, \varphi_P, \varphi_2') \quad (7)$$

$$f_F(u_F, \theta_F, \varphi_F) = 0 \quad (8)$$

$$f_P(u_P, \theta_P, \varphi_P) = 0 \quad (9)$$

$$\underline{n}_f^{(1)}(\theta_F, \varphi_F, \varphi_1') = \underline{n}_f^{(2)}(\theta_P, \varphi_P, \varphi_2') \quad (10)$$

Here, φ_1' and φ_2' are the angles of rotation of gears 1 and 2, respectively, when they are in mesh; φ_F and φ_P are the angles of rotation of the generating gears.

The equations of meshing (eqs. (8) and (9)) are linear in u_F and u_P respectively. Eliminating u_F and u_P , we may represent equations (7) to (9) as follows:

$$\underline{r}_f^{(1)}(\theta_F, \varphi_F, \varphi_1') = \underline{r}_f^{(2)}(\theta_P, \varphi_P, \varphi_2') \quad (11)$$

Equations (10) and (11), considered simultaneously, express that when surfaces Σ_1 and Σ_2 are in mesh, they have a common point and a common normal, and that such a point is the contacting point of the gear tooth surface. Since equations (10) and (11) are vector equations, there is a total of six scalar equations. Because the surface normal vectors are unit vectors, there are only five independent scalar equations in six unknowns. Fixing one of the six unknowns in these equations (say θ_F), we may solve the system for the other parameters as functions of θ_F . This may be represented as follows:

$$\theta_P(\theta_F), \quad \varphi_F(\theta_F), \quad \varphi_P(\theta_F)$$

$$\varphi_1'(\theta_F), \quad \varphi_2'(\theta_F)$$

The equations are solved using a nonlinear equation solver which is based on an iterative scheme. The kinematic error is determined simply by comparing the rotations φ_1' and φ_2' .

Bearing Contact

The determination of the dimensions and orientation of the contacting ellipse at the contacting point is based on the method developed by Litvin (refs. 1, 2, and 12). The method starts with the equation for the normal curvature which comes from differential geometry theory.

$$K_n = \frac{\dot{n} \cdot v}{v^2}$$

where K_n is the normal curvature, v is the velocity of the contact point in motion along the surface and \dot{n} is the velocity of the tip of the surface unit normal, \underline{n} , which changes its direction while the point moves over the surface.

The method of finding the contact ellipse is further developed by the following considerations in solving a characteristic value (eigenvalue) problem. The maximum and minimum values of curvatures are the "principal" values of curvature and the principal directions are the corresponding directions of the unit vectors that are tangent to the line of intersection formed by the normal plane and the surface whose curvature is sought. The method is to determine the principal curvatures and directions of surfaces Σ_1 and Σ_2 in terms of the principal curvatures and directions of the generating surfaces Σ_F and Σ_P . Then the relations between the principal curvatures and direction of the contacting surfaces are used to determine the contact ellipse of the elastically deformed tooth surfaces.

Consider that the principal curvatures and directions for the contacting surfaces are determined and P (fig. 8) is the point of contact of gear tooth surfaces and the unit vectors $\underline{i}_I^{(2)}$ and $\underline{i}_I^{(1)}$ represent principal directions $I^{(1)}$ on gear tooth surfaces, Σ_1 and Σ_2 . Principal direction $II^{(1)}$ is perpendicular to the unit vector $\underline{i}_I^{(1)}$ ($I = 1, 2$). Unit vectors $\underline{i}_I^{(2)}$ and $\underline{i}_I^{(1)}$ lie in the tangent plane to surfaces Σ_2 and Σ_1 which is drawn through the instantaneous contact point P . Angle $\sigma^{(21)}$ which is formed by unit vectors $\underline{i}_I^{(2)}$ and $\underline{i}_I^{(1)}$ is known since the principal directions for the mating surfaces have already been determined.

Axes $2a$ and $2b$ of the contact ellipse represent its dimensions and angle α its orientation with respect to $\underline{i}_I^{(2)}$. Angle α is measured counter-clockwise from the n -axis to $\underline{i}_I^{(2)}$. We may determine a , b , and α using the following equations (12):

$$A = \frac{1}{4} \left[K_c^{(1)} - K_c^{(2)} - \left(g_1^2 - 2g_1g_2 \cos 2\sigma^{(21)} + g_2^2 \right)^{1/2} \right]$$

$$B = \frac{1}{4} \left[K_e^{(1)} - K_e^{(2)} + \left(g_1^2 - 2g_1g_2 \cos 2\sigma^{(21)} + g_2^2 \right)^{1/2} \right]$$

$$a = \left(\left| \frac{\delta e}{A} \right| \right)^{1/2} \quad b = \left(\left| \frac{\delta e}{B} \right| \right)^{1/2} \quad (12)$$

$$\tan 2\alpha = \frac{g_2 \sin 2\sigma^{(21)}}{g_1 - g_2 \cos \sigma^{(21)}}$$

where

$$K_e^{(1)} = K_I^{(1)} + K_{II}^{(1)}, \quad \text{and} \quad g_1 = K_I^{(1)} - K_{II}^{(1)} \quad (1 = 1, 2)$$

δ_e is the approach of the elastic surfaces under the load. The bearing contact is simply the envelope of the set of contact ellipses for the entire meshing cycle of the mating teeth. The new generating process lets the contact ellipse move lengthwise along the tooth, with the major axis of the contact ellipse being generally transverse to the contact path. This is the best motion to encourage good development of a lubrication film.

NUMERICAL EXAMPLE

Figure 9 shows the bearing contact on the convex side of the gear tooth in a set of bevel gears with the following parameters:

| | |
|--------------------------|---|
| tooth numbers | $N_1 = 10 \quad N_2 = 41$ |
| gear pressure angle | $\psi_c^{(P)} = 20^\circ$ |
| diametral pitch | $P_d = 141.2 \text{ mm (5.559 in.)}$ |
| mean cone pitch distance | $O_h N = 81.94 \text{ mm (3.226 in.)}$ |
| pinion cutter radius | $r_c^{(F)} = 76.175 \text{ mm (2.999 in.)}$ |
| gear cutter-radius | $r_c^{(P)} = 73.15 \text{ mm (2.88 in.)}$ |
| | $\Delta E_1 = -1.27 \text{ mm (-0.0499 in.)}$ |
| | $\Delta L_1 = -0.93 \text{ mm (-0.0368 in.)}$ |

The contact ellipse moves along the surface in the process of meshing. The kinematic error is zero over the whole mesh cycle if the pinion cutter blade angle, $\psi_c^{(F)} = 16.969^\circ$ and $\delta = -0.274^\circ$. However this blade angle is not practical. Choosing the nearest blade angle $\psi_c^{(F)} = 17^\circ$ requires also that $\delta = -0.314^\circ$ and hence, results in nonzero kinematic errors, but they are still very small. For this example, they are less than 0.02 arc sec. For gears made without the special machine settings, the kinematic errors are in the range from 20 to 90 arc seconds.

SUMMARY OF RESULTS

Spiral bevel gear geometry was investigated using the standard laws of kinematics for spatial gearing, as well as important results from the differential geometry field. The object was to eliminate kinematic errors in the motion transmission because such errors are a major source of noise and vibration. A computer program was created that simulates the cutting and meshing processes for the pinion and gear. The computer program yielded the tooth geometry, contact path, kinematic error, and contact ellipse between the mating gear teeth.

The following results were obtained.

1. A new method for generation of spiral bevel gears with zero kinematical error was developed. Gleason gear generating equipment may be used. Practical considerations of using standard blade angles give nonzero but still very small kinematic errors.
2. The new generation method was confirmed by calculations run on a digital computer program for tooth contact analysis.
3. The generation process takes place under the requirement of a constant direction for the contact normal during the process of meshing. The process may be imagined as if the tooth surface normal is carried by two mating ellipses.
4. The new process provides that the contact ellipse moves lengthwise along the tooth in the most advantageous way for good lubrication.

REFERENCES

1. Litvin, F.L.: The Theory of Gearing. 2nd edition, Nauka, Moscow, 1968. (In Russian)
2. Litvin, F.L.; Rahman, P.; and Goldrich, R.N.: Mathematical Models for the Synthesis and Optimization of Spiral Bevel Gear Tooth Surfaces for Helicopter Transmissions. NASA CR-3553, 1982.
3. Litvin, F.L.; and Coy, J.J.: Spiral-Bevel Geometry and Gear Train Precision. Advanced Power Transmission Technology, NASA CP-2210, G.K. Fischer, ed., 1983, pp. 335-344.
4. Litvin, F.L., et al: Synthesis and Analysis of Spiral Bevel Gears. Design and Synthesis; H. Yoshikawa, ed., North Holland, 1985, pp. 302-305.
5. Litvin, F.L., et al.: Generated Spiral Bevel Gears: Optimal Machine-Tool Settings and Tooth Contact Analysis. NASA TM-87075, 1985.
6. Litvin, F.L.; and Gutman, Y.: Methods of Synthesis and Analysis for Hypoid Gear-Drives of "Formate" and "Helixform," Parts 1-3. J. Mech. Des., vol. 103, no. 1, Jan. 1981, pp. 83-113.
7. Litvin, F.L.; and Gutman, Y.: A Method of Local Synthesis of Gears Grounded on the Connections between the Principal and Geodetic Curvatures of Surfaces. J. Mech. Des., vol. 103, no. 1, Jan. 1981, pp. 114-125.
8. Tooth Contact Analysis, Formulas, and Calculation Procedures. The Gleason Works, Rochester, NY, Publication No. SD3115, 1964.
9. Understanding Tooth Contact Analysis. The Gleason Works, Rochester, NY, Publication No. SD3139, 1981.
10. Hart, H.J., et al: "Bevel- and Hypoid-Gear Manufacture." Chapter 20 Gear Handbook: The Design, Manufacture, and Application of Gears, D.W. Dudley, ed., McGraw-Hill, 1962.
11. Townsend, D.P.; Coy, J.J.; and Hatvani, B.R.: OH-58 Helicopter Transmission Failure Analysis. NASA TM-X-71867, 1976.
12. Litvin, F.L.: Die Beziehungen Zwischen den Krümmungen der Zahnoberflächen bei Räumlichen Verzahnungen, Z. Angew. Math. Mech., vol. 49, no. 11, 1969, pp. 685-6990 (in German). Relationships Between the Curvatures of Tooth Surfaces in Three-Dimensional Gear Systems. NASA TM-75130.

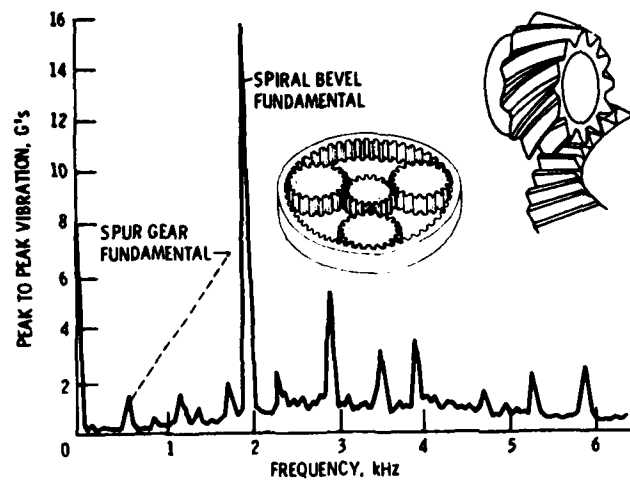


Figure 1 - Transmission vibration spectrum.

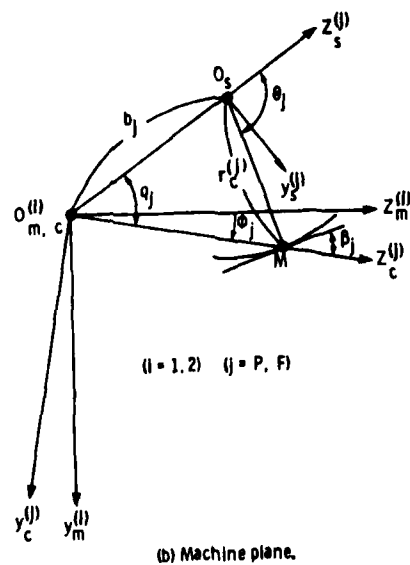
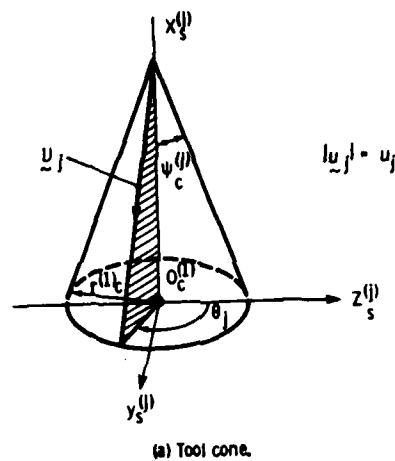


Figure 2 - Machine settings.

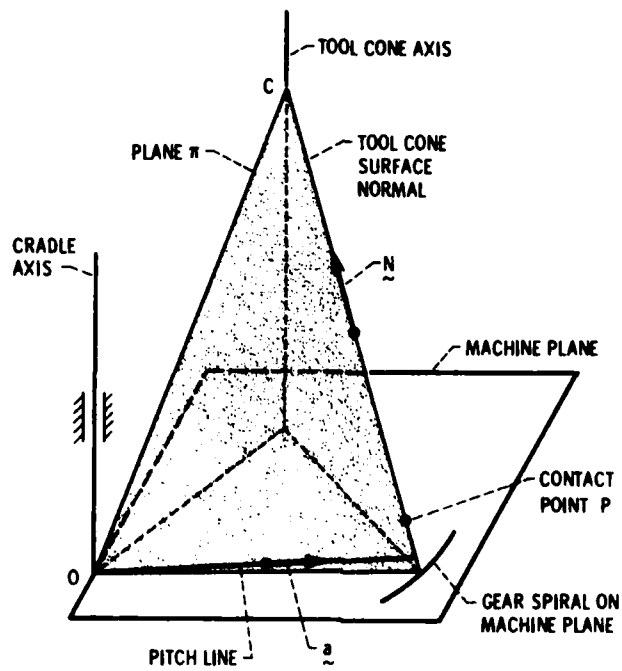


Figure 5. - Definition of plane π .

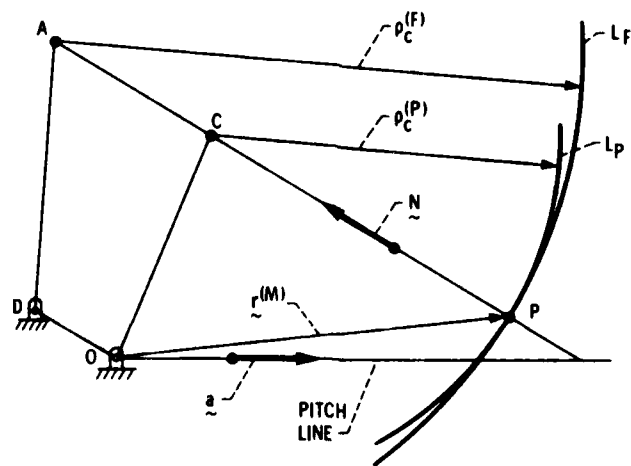
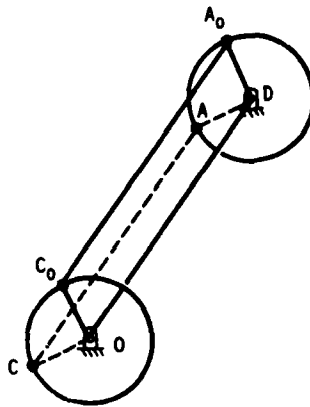
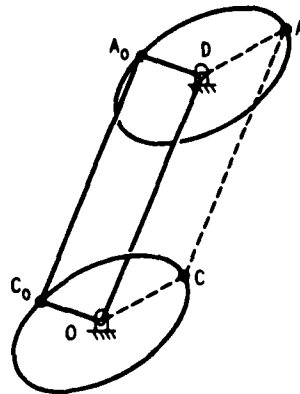


Figure 6. - Meshing in plane π .



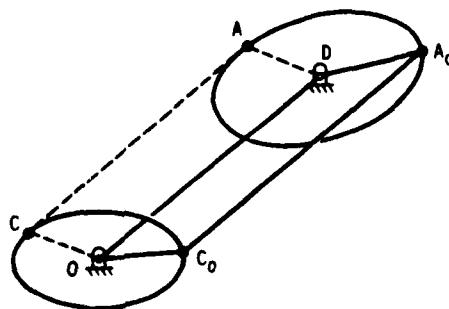
(a) With a simple 4-bar linkage.

Figure 7. - Achieving parallel motion for link CA.



(b) With identical ellipses.

Figure 7. - Continued.



(c) With mating ellipses.

Figure 7. - Concluded.

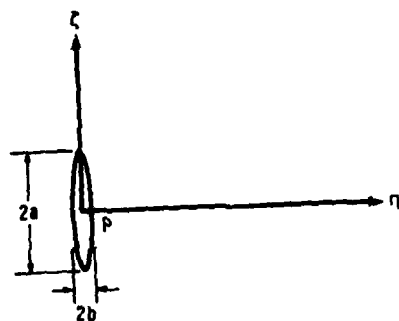
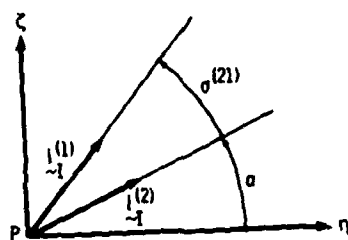


Figure 8. - Contact ellipse and principal directions.

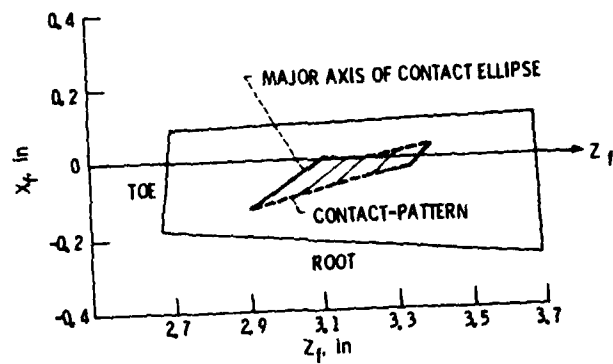


Figure 9. - Contact pattern - the envelope of contact ellipses.
 $\psi_c^{(P)} = 20^\circ$; $\psi_c^{(F)} = 17^\circ$; convex side of tooth.

| | | | | | |
|---|--|--|--|---|--|
| 1 Report No NASA TM 87273 USAAVSCOM TR 86 C 2 | | 2 Government Accession No. | | 3 Recipient's Catalog No. | |
| 4 Title and Subtitle Generation of Spiral Bevel Gears With Zero Kinematical Errors and Computer Aided Tooth Contact Analysis | | | | 5 Report Date March 1986 | |
| | | | | 6 Performing Organization Code | |
| 7 Author(s) Faydor L. Litvin, Wei-Jiung Tsung, John J. Coy, and Charles Heine | | | | 8 Performing Organization Report No. E. 2932 | |
| | | | | 10 Work Unit No. | |
| 9 Performing Organization Name and Address NASA Lewis Research Center and Propulsion Directorate, U.S. Army Aviation Research and Technology Activity - AVSCOM, Cleveland, Ohio 44135 | | | | 11 Contract or Grant No. | |
| | | | | 13 Type of Report and Period Covered Technical Memorandum | |
| 12 Sponsoring Agency Name and Address National Aeronautics and Space Administration Washington, D.C. 20546 and U.S. Army Aviation Systems Command, St. Louis, Mo. 63120 | | | | 14 Sponsoring Agency Code | |
| | | | | | |
| 15 Supplementary Notes This material is similar to that presented at the 2nd World Congress on Gearing, Paris, France, March 2-5, 1986. Faydor L. Litvin and Wei-Jiung Tsung, University of Illinois at Chicago, Chicago, Illinois; John J. Coy, Propulsion Directorate, U.S. Army Aviation Research and Technology - AVSCOM; Charles Heine, Dana Corporation, Fort Wayne, Indiana. | | | | | |
| 16 Abstract A new method for the generation of Gleason's spiral bevel gears which provides conjugated gear tooth surfaces and an improved bearing contact has been developed. A computer aided program for the simulation of meshing, misalignment, and bearing contact has been developed. | | | | | |
| 17 Key Words:(Suggested by Author(s)) Spiral bevel gears; Mechanisms; Vibrations; Noise, Machine design. | | | | 18 Distribution Statement Unclassified - unlimited SIAR Category 37 | |
| 19 Security Classif. (of this report) Unclassified | | 20 Security Classif. (of this page) Unclassified | | 21 No. of pages | |
| | | | | 22 Price* | |

END

DTIC

6-86